Huifen Liang[1], Jason Blake Cohen[2*]

[1]School of Atmospheric Sciences, Sun Yat-Sen University, Zhuhai, 519000, China

[2]School of Environment and Spatial Informatics, China University of Mining and Technology, Xuzhou, 221000, China

Corresponding author: Jason Blake Cohen (jasonbc@alum.mit.edu; wjjs0011@cumt.edu.cn)

Key Points:

- Solar UV Radiation is found to be the most important factor driving surface ozone.
- Ozone is produced well under both polluted and clean conditions, including both high and low $PM_{2.5}$ and CO conditions.
- Ozone is well produced temporally across nine very different urban areas using the same big-data derived approach.

Abstract

This work constructs multiple regression equations of surface ozone concentration based on non-linear combinations of high temporal frequency and multi-year measurements of air pollutant concentrations ($PM_{2.5}$, CO, NO_2, SO_2) and remotely sensed ultraviolet Index (UVI) in nine different urban regions in China. These nine regions all have different emissions profiles, economic drivers, and climatology, allowing a more rigorous investigation of the factors most responsible to local surface ozone. The results show a good fit of ozone can be made temporaly (including many peaks and troughs), under conditions ranging from relatively clean through polluted, with minimum and maximum bounds on the goodness of the fit usually in the range from 5 to 130 g/m^3. Overall, the results demonstrate significant differences in terms of the most important driving factors in the different cities, with UV radiation being most important in all cities, followed by CO, $PM_{2.5}$, and NO_2 or a combination, depending on each individual city. The performance of the ozone prediction and real measurements under both clean and polluted conditions of $PM_{2.5}$ or CO mass concentrations are further explored and found to match very well in Xi'an and Beijing. Discussion is presented and supported to quantify insights into why solar ultraviolet radiation coupled with easier to measure longer-lived air pollutants contribute a significant amount to surface ozone is possible, all without needing to necessarily at first order wade into the extremely complex chemistry and physics involved with boundary layer meteorology and VOC chemistry.

Plain Language Summary

Since ozone is both an air pollutant and a greenhouse gas, understanding its atmospheric concentration is very important. However, measurements of surface ozone are highly difficult to obtain from remotely sensed platforms, requiring

surface stations running at high frequency. Since ozone is not directly emitted, any simple relationship between drivers and concentrations is complex. To this end, many studies have worked to either address the complex chemistry in high detail, or to make a simple set of linear approximations using big data. This work aims to strike a balance between these two positions, using both large-data sets and some form of non-linear chemistry, and fitted over nine very different urban regions with vast ranges of emissions factors, economics, geography, and meteorology. Overall, this work finds that solar UV radiation is the single most important factor in terms of understanding and predicting surface ozone, which while supported by theory, tends to be less considered in general. Overall, this works finds that a good representation can be made under conditions ranging from clean through polluted. The non-linear impacts of co-emissions of $PM_{2.5}$ and CO are also explored, and open further discussions into applications of this approach to possible future mitigation strategies.

1 Introduction

Tropospheric Ozone (O_3) is a secondary gaseous species produced from photochemical reactions including CO, VOCs, and NO_x (Seinfeld and Pandis, 1998). Due to its absorption in the infrared range, tropospheric ozone is a short-lived greenhouse gas, with an estimated radiative forcing in the range of 0.32-0.62W/m^2 during the period from 1850 to 21st century (Brasseur et al., 1998; Rap et al., 2015; Sitch et al., 2007; Skeie et al., 2020). Ozone has also been found to be detrimental to human health and agriculture (Lu et al., 2020; Wang et al., 2017). Over the period from 2013 to 2017, surface ozone measurements of large amounts of cities in China are observed to be increasing. This time period corresponds to the first year when China developed and implemented multiple policies making efforts to find ways to reduce fine particle matter. In this period a tremendous amount of progress has been made since this time to reduce anthropogenic emissions of directly and indirectly emitted species, with a focus on reducing the surface concentration of $PM_{2.5}$ (Wang et al., 2019). It has been demonstrated clearly that the $PM_{2.5}$ concentration has decreased in many tier 1 and tier 2 cities in coastal and more developed regions of China, along with certain precursors of $PM_{2.5}$ including NO_2 and SO_2 (Cheng et al., 2019; Liu & Wang, 2020).

However, even with all of this successes, tropospheric ozone has been observed on average to not decrease. Furthermore, high ozone days have been found to occur more frequently (K. Li et al., 2019; Ke Li et al., 2019; Lu, Hong, et al., 2018; Y. Wang et al., 2020). This is a common phenomenon also found to be the case in many urban areas of the developed world such as the Northeastern USA, Western Europe, and Japan, where ozone levels have proven stubborn to lower based solely on policies meant to reduce $PM_{2.5}$ (Liao, 2008; Lu, Hong, et al., 2018). There are many possible reasons for this, including: an increase of solar radiation reaching at surface due to reductions in $PM_{2.5}$ (Cohen & Prinn, 2011; Pan et al., 2019; Wu et al., 2020), non-linear chemistry of NO_x (Wu et al., 2009), biogenic VOCs (Li et al., 2013; Wang et al., 2008), and long term changes

in OH (Prinn et al., 2005). It is believed that the increase of surface ozone is due in part to the changes in ultraviolet radiation as a function of $PM_{2.5}$.

To this end, there have been very few studies which have looked at the impact of changes in solar radiation on ozone formation, especially so from an environmental management perspective (Belan & Sklyadneva, 1999; Liu et al., 2019). A small portion of incoming solar radiation, is at wavelengths smaller than 400nm, called solar ultraviolet radiation (UVR). While small amounts of UVR are beneficial for people, specifically with respect to Vitamin D production and aiding in the treatment of certain diseases, in general long-term exposure to UVR may cause damage to the human body (Cadet et al., 2020; WHO, 2020). Generally UVR is divided into 3 bands according to different wavelengths and energy levels: UVC(100-280nm), UVB(280-315nm), and UVA(315-400nm), with all UVC and a large portion of UVB being absorbed or scattered by atmospheric ozone, water vapor, oxygen, nitrogen, black carbon aerosol, and clouds, among others, leaving a small part of UVB and a moderate part of UVA emitted from the sun that actually can reach the Earth's surface (Engelsen et al., 2005; Wang, Wang, et al., 2021; WHO, 2020). It is these energetic wavelengths which are the key driver of the photochemistry impacting ozone, as well as also being a major driver behind photochemical reactions of many various relatively stable molecules into more reactive fragments in the troposphere (Tang et al., 2011).

Long term average concentrations of $PM_{2.5}$ (atmospheric fine particulate matter with aerodynamic diameter less than or equal to 2.5 m) in China has been observed at extremely high levels over a considerable amount of time over the last two decades, attracting widespread attention due to its harmful impacts on visibility, human health (mental and physical health), traffic safety, construction, economy , nature, and its interaction with climate (Liang et al., 2016). Previous studies have pointed out that coal combustion, motor vehicle emissions and industrial sources are major $PM_{2.5}$ sources in China, while domestic fuel burning, biomass burning, other anthropogenic emissions sources, as well as dust also contribute to $PM_{2.5}$ concentration in China as well (Cohen & Wang, 2014; Huo et al., 2011; Karagulian et al., 2015; Wang, Cohen, et al., 2021; Zhang et al., 2007). $PM_{2.5}$ comprises of inorganic sources such as sulfate, nitrate, and mineral dust, and organic sources such as organic carbon and black carbon (BC), with the portion of these components varying in degree based on the day of the year, source time, geographic region, and local meteorology, among other factors (Deng et al., 2021; Ding et al., 2016; Wang, Wang, et al., 2021).

$PM_{2.5}$ can lead to a decrease in solar radiation reaching at surface through a combination of scattering and absorption, which are in determined by the $PM_{2.5}$ concentrations in the air, its chemical composition, its size distribution, its hygroscopic potential and water vapor, its vertical distribution, the land surface properties, meteorology, and more (Guo et al., 2019; Holben et al., 1998; Hu et al., 2017; Huang et al., 2014; Tao et al., 2017; Wang et al., 2015; Xu et al., 2020; Zhang et al., 2015). Scattering of solar radiation decreases the direct visible light intensity at the surface, thereby leading to issues with visibility and

surface temperature change, while the absorption may increase the temperature at the height of the aerosol layer and thus generate effects on meteorology and precipitation among other issues (Hill & Ming, 2012; Ramanathan et al., 2001). It is also noted that scatter/absorption of $PM_{2.5}$ may inhibit/favor photochemical and temperature sensitive reactions respectively in the lower troposphere through decreasing the radiation intensity or increasing the temperature in the aerosol layer.

Satellite-based remote sensing can be used to measure atmospheric ozone based on absorption in both UV and infrared bands. Some instruments, such as the Nimbus Total Ozone Mapping Spectrometer (TOMS), the Aura Ozone Monitoring Instrument (Huang et al.), and Global Ozone Monitoring Experiment (GOME), etc., can derive ozone amounts and its vertical profiles in the stratosphere, while in general tropospheric ozone detection is less sensitive (Bak et al., 2012; Liu et al., 2004; Martin, 2008; Miyazaki et al., 2019), due to the fact that the majority of the vertically integrated O_3 column is found in the stratosphere. At the present time, the best remote sensing can generally do for tropospheric ozone is to make observations of the lower troposphere (not only confined to the surface or the boundary layer) over highly polluted regions, in which case there still remains a large bias (of or greater than 10%) with respect to measurements (Liu et al., 2005; Kajino et al., 2019). There are also point-measurements made by upward looking O_3 LIDAR, but these results are highly limited in space and also tend to also be error prone (Steinbrecht et al., 2009; H. Wang et al., 2020).

The concentration of ozone in the troposphere is controlled by a complex balance between different forms of organics, nitrogen, hydrogen, oxygen, UV radiation, and thermodynamics, as compared to being directly emitted. In specific, the concentration of ozone is related to the atmospheric concentrations of CO, NO_2, and SO_2 (all of which have high frequency surface measurements readily available) specifically via the HO_x and NO_x cycles. Furthermore, it is known that the second-to-last step in the chain is directly related to UV radiation cleaving the O radical from the NO_2 to finally form Ozone, and therefore is also directly related to measurements of UV radiation (such as UVI). Due to the interactions between aerosols and UV radiation, and the high amount of availability of measurements, $PM_{2.5}$ is also used in this study. In specific, this work constructs a surface O_3 prediction based directly upon measured concentrations of $PM_{2.5}$, CO, NO_2, SO_2, UVR, and a subset of their non-linear terms in terms of UVR.

This paper takes a similar approach of using simple models grounded in physical and chemical understanding, and then applying these large datasets of measurements to construct a response and analyze its impacts, as demonstrated in other recent papers relating to fire plume height (S. Wang et al., 2020), biomass burning geospatial sources (Cohen, 2014), and the 3-D emissions profile of CO (Lin et al., 2020). The idea is to reach a deeper understanding that can be further integrated into intense and detailed models, or used for policy and other downstream analysis, with a modeling system which is more physically and chemically realistic as compared with a pure big-data approach (Wei et al., 2021), yet still

is fully grounded in approximately 4 million individual measurements of O_3 and another similar number of individual measurements of each of its precursor species. Additionally, each precursor's contribution to local ozone is explored as a function of geography, UVR intensity, and $PM_{2.5}$ levels, including quantification of uncertainty. Finally, possible reasons for the results have been discussed in the following sections.

2 Methodology and Data

The goal is to use high frequency measurements to allow for the reproduction of both daily-to-weekly frequency events that are relatively polluted and relatively clean. The non-linear terms aim to analyze the effects of each pollutant gas and particle measured on how its concentration may interfere with or change the UVR, as supported by the theory and modelling papers previously introduced. Therefore, from a measurement perspective, we aim to find a way to analyze the effects in the real world on the real-world measurements of O_3 at the ground level, based on both analytics of large data sets as well as on physical underlying models.

2.1 Approximating Ozone Formation

The concentration of ozone in the atmosphere is effectively and fundamentally the chemical balance between UV moderated photolysis, the HO_x cycle, the NO_x cycle, and carbon in the atmosphere. The photochemistry of Ozone is well established by (Seinfeld & Pandis, 1998; Tang et al., 2011), with its main reactions shown in **Equations 1a-1i**. With the key initiating reaction of ozone photolysis with UVR (shown as h in **Equations 1a** and **1h**), one of the products, electronically excited oxygen atoms, $O(^1D)$, react with H_2O to further produce hydroxyl radicals ($\cdot OH$). This product, which is an essential cleaning agent of the atmosphere for gasses such as NO_2, SO_2, VOCs and CO, **Equations 1c~1f** (Wang & Prinn, 2000), produces HO_2 through series of cleaning reactions. HO_2 further oxidizes NO into NO_2, which further photolyzes under the radiation of wavelengths less than 420nm to produce odd oxygen atoms ($\cdot O$), and further produces Ozone in the troposphere.

$$O_3 + \mathrm{h}\ (\lambda < 320\mathrm{nm}) \rightarrow O(^1D) + O_2 \quad (1a)$$

$$O(^1D) + H_2O \rightarrow \bullet\mathrm{OH} + \bullet\mathrm{OH} \quad (1b)$$

$$\bullet\mathrm{OH} + \mathrm{NO_2} \rightarrow \mathrm{HNO_3} \quad (1c)$$

$$\bullet\mathrm{OH} + \mathrm{SO_2} \rightarrow ... \rightarrow \mathrm{HO_2} + H_2\mathrm{SO_4} \quad (1d)$$

$$\bullet\mathrm{OH} + \text{hydrocarbons} \rightarrow \mathrm{HO_2} + \text{partly oxidated organics} \quad (1e)$$

$$\bullet\mathrm{OH} + \mathrm{CO} \xrightarrow{O_2} \mathrm{HO_2} + \mathrm{CO_2} \quad (1f)$$

$$\mathrm{HO_2} + \mathrm{NO} \rightarrow \bullet\mathrm{OH} + \mathrm{NO_2} \quad (1g)$$

$$\mathrm{NO_2} + \mathrm{h}\ (\lambda < 420\mathrm{nm}) \rightarrow \mathrm{NO} + \bullet O \quad (1h)$$

$$\bullet O + O_2 \rightarrow O_3 \quad \text{(1i)}$$

Generally, the concentration of O_3 in the troposphere is affected by meteorological conditions like temperature, humidity, wind, UVR, and concentrations of various chemicals including $PM_{2.5}$, NO_x, SO_2, CO and VOCs, as demonstrated in Chinese urban and downwind areas by (Cohen et al., 2011; Li et al., 2021; Wang et al., 2017). The fundamental measurements, techniques, and approaches used to approximate surface ozone concentration in this work are described below.

2.2 Chemical Concentration Measurements

Atmospheric concentrations of $PM_{2.5}$, CO, NO_2, O_3, and SO_2, with unit of g/m^3 are measured and recorded hourly by the China National Environmental Monitoring Center at 1718 Distinct stations. This work specifically uses all of the available data from the 92 stations found within the urban, suburban, and rural parts of the following 9 cities: Beijing, Shanghai, Wuxi, Chengdu, Chongqing, Guangzhou, Xi'an, Taiyuan, and Jiaozuo. All observations are used which are available starting from 1 January 2014 through 31 December 2018. In this work, daily average values are computed and subsequently used, with statistics of the daily average climatological mean and standard deviation across the various stations given in Supplemental **Tables A1** and **A2**.

2.3 OMI Ultraviolet Measurements

Ultraviolet Index (UVI) was adopted as a standard indicator of solar ultraviolet (UV) levels by the World Meteorological Organization and World Health Organization in 1994. UVI quantitively describes the amount of integrated total solar ultraviolet radiation at the Earth's surface (World Health Organization, 2002), which is a unitless quantity starting from 0 when there is no UV radiation present, and increasing with UV intensity.

In this study, the daily UV Index was obtained from the daily OMI satellite product OMUVBG, at a spatial resolution of 0.25 degree x 0.25 degree, over the time from 1 January 2014 through 31 December 2018. Previous studies have shown that UVI decreases with increasing latitude, consistent with the theory of the atmospheric pathlength extinction of UV radiation. For this reason, coupled with the fact that higher elevations have a thinner atmospheric pressure, the highest UVI value occurs at high altitude sites in the tropics (e.g., at Reunion Island (21°S, 55°E) and at Hawaii UVI has been observed of about 20 while Satellite-based estimates of UVI value are more than 25) (Cadet et al., 2020). Using these results to ensure that the results are valid (quality controlled), in this work all values of UVI greater than 20 are regarded as missing values, consistent with the maximum values in Hawaii and the most equatorial region of this study being located at about 23°N. A statistical summary of the UVI data in terms of daily average mean and standard deviation are given in Supplemental **Table A3**.

2.4 Geography

Given that urban areas tend to have a much larger range of values of ozone, encompassing both background and active chemical production conditions, as well as larger populations to be impacted by ozone, an ideal model of surface ozone should be able to reproduce values in urban regions at reasonably high frequency and over the range of conditions present. Furthermore, due to the impacts of cloud-cover, the atmospheric water cycle, AOD, and temperature on UV radiation and ozone reaction rates, it is essential for vastly different geographic regions to also be considered if a successful model is to be constructed. On top of this, it is hoped that by considering a wide-enough range of conditions that the model may potentially be generalizable in the future. For these reasons, we choose 9 large urban sites in China with varying degrees of economic development and emissions, high population density, and various climatological chemical and meteorological forcings. In specific the areas selected include: Beijing, Shanghai, Wuxi, Chengdu, Chongqing, Guangzhou, Xi'an, Taiyuan and Jiaozuo as displayed in **Figure 1**. To address the heterogeneous nature of these urban areas, data have been selected from both central city measurement sites, as well as from those in outer regions which have lower ozone loadings and different emissions profiles, but are still quite chemically active due to local and long-range transport of the subset of moderate to longer-lived ozone precursors.

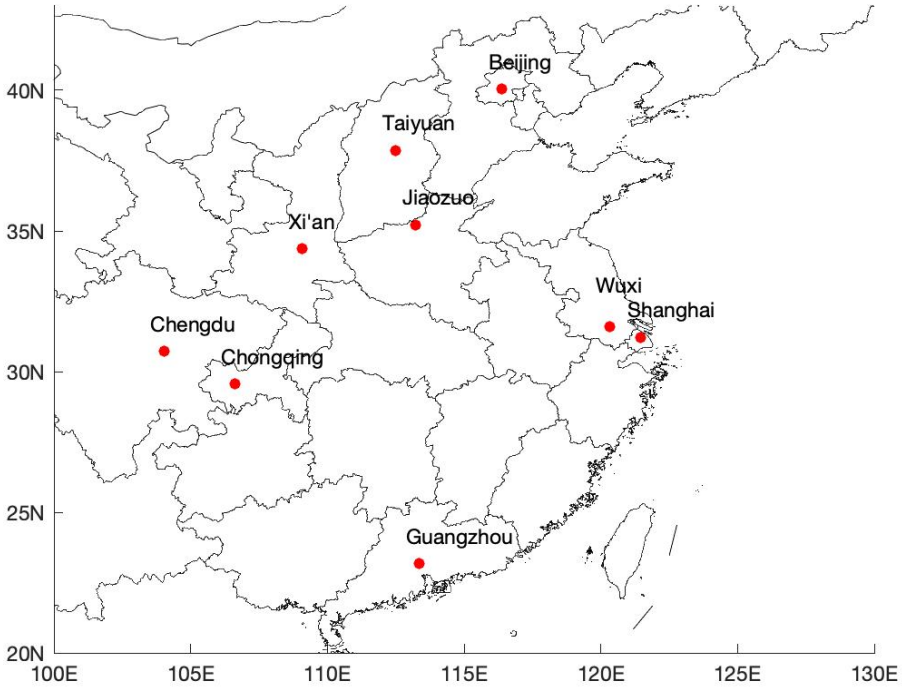

Figure 1. Locations investigated in this study.

2.5 Statistics and Analytics

Multiple statistical methods were used in this study to connect the concentration measurements of those species factors which drive ozone formation and transport, with the measured concentrations of surface ozone. Multiple linear equations are used to approximate ozone compiled on the basis of measured values of $PM_{2.5}$, CO, NO_2, SO_2 and UVI were built and tested following the approach in (S. Wang et al., 2020). To accommodate both simple linear reactions, as well as the fact that multiple reactions involve concentrations of both chemical species as well as the UV available flux, additional non-linear terms have also been added. In specific, these linear and a first order non-linear terms are used in a manner so as to include all possible logical combinations from the basic chemical theory, particularly those between UV radiation and chemicals which are UV sensitive. For this reason, the sets of equations employed in this work are shown based on **Equations 2a** (linear) and **2b** (linear plus non-linear) below,

$$O_3 = b_1 \times \mathrm{PM}_{2.5} + b_2 \times CO + b_3 \times \mathrm{NO}_2 + b_4 \times \mathrm{SO}_2 + b_5 \times UVI \quad (2a)$$

$$O_3 = b_{11} \times \mathrm{PM}_{2.5} + b_{21} \times CO + b_{31} \times \mathrm{NO}_2 + b_{41} \times \mathrm{SO}_2 + b_{51} \times UVI + b_{12} \times \mathrm{PM}_{2.5} \times UVI + b_{22} \times CO \times UVI + b_{32} \times \mathrm{NO}_2 \times UVI + b_{42} \times \mathrm{SO}_2 \times UVI \quad (2b)$$

where the terms b_i, b_{ij}, (etc.) are the values which are meant to be fit based on the measurements and which depict the magnitudes of the various different driving forces underlying the contributions of those processes to the total measured surface O_3 concentrations.

To determine which least squares fits are most ideas, a set of specific quantitative statistics are generated, including the coefficient of determination (R^2), the Root Mean Squared Error (RMSE), and the correlation between the derived equations and original surface ozone measurements. These equations were analyzed assuming a value of $p<0.05$.

Analytical techniques employed when comparing the results from the simple model to those across different measurements include simple statistics as well as Probability Distribution Functions (PDFs). In specific, the range of the modeled outputs is considered important as a means of evaluating the region over which the fit can be trusted. In general, knowledge of any upper or lower cutoff bounds provide guidance as to whether or not the approach may have practical use in the real world. Furthermore, specific levels of bias are also determined, so that a deeper understanding of what steps may be taken to improve upon this work can be subsequently investigated.

3 Results

3.1 Multiple Regression Equations of Ozone Using Linear and Non-linear Terms

One of the simplest chemical systems capable of representing the ozone concentration is given by **Equations 1a~1i**. As expected from the complexity

of **Equations 1a~1h**, forming a specific relationship between non-linear terms and ozone is not likely to be sufficient to be fully predicted across a broad range of concentrations, even though most previous attempts at using big-data have done exactly this (Tie et al., 2009; von Kuhlmann et al., 2003). Therefore, this work builds a relationship between the forcing terms $PM_{2.5}$, CO, NO_2, SO_2, UVI and the selected first order non-linear terms $PM_{2.5}$*UVI, CO*UVI, NO_2*UVI and SO_2*UVI, as given by **Equations 2a**,**2b**. The reason for choosing these non-linear terms with respect to UVI and a chemical concentration is that the PSSA (photochemical steady state assumption) only holds true when both the chemical concentration and the actinic flux of active radiation are both well constrained (Seinfeld et al., 2003).

The coefficients of these terms, including both first order linear and non-linear contributions were fitted using a least squares optimization, with the statistics of the best fitting cases listed for each site in (**Table 1**). These results are the ones subsequently used to build the model results herein. However, to determine which the goodness of the modeled solutions, a combination of computed R^2 (temporal goodness of fit) and RMSE (magnitude goodness of fit) are both applied. The resulting fits are demonstrated to be especially good in Xi'an, Chongqing, and Chengdu, which consistently have R^2 values larger than 0.489 and RMSE values smaller than 19.8 g/m^3, which are considered very good based on the measurement errors associated with the data from this network as given in Guo et al. (2019) and Liang et al. (2021). Those stations located in extremely urban and spread-out areas tend to have R^2 values which are less good, with the values in Shanghai and Wuxi, all having an R^2 less than 0.36, and the RMSE at these stations is worse than that of other sites, ranging from 25.0 to 25.8 g/m^3. This is consistent with the complex chemical environments from multiple anthropogenic sources and even many of the best transport models also showing disparities in the timing and location of peak ozone concentrations in highly urban areas, while in generally still matching the magnitudes reasonably well (Abdi-Oskouei et al., 2020; Visser et al., 2019).

Table 1

Coefficients and Statistical Data of the Regression Equations (Units: b_{ij} and R^2: unitless (i=1,2,3,4, j=1,2); b_{51} and RMSE: g/m^3).

	$\mathbf{b_{11}}$	$\mathbf{b_{21}}$	$\mathbf{b_{31}}$	$\mathbf{b_{41}}$	$\mathbf{b_{51}}$	$\mathbf{b_{12}}$	$\mathbf{b_{22}}$	$\mathbf{b_{32}}$	$\mathbf{b_{42}}$	$\mathbf{R^2}$
Beijing	0.0440	-0.0168	0.929	-0.854	18.5	0.0402	1.66E-3	-0.392	0.346	0.442
Shanghai	-0.950	0.130	-0.332	-0.300	16.1	0.263	-0.0275	-0.0303	-1.78E-3	0.231
Wuxi	-0.722	0.0520	-0.0111	0.454	11.8	0.189	-8.89E-3	-0.0684	-0.147	0.357
Chengdu	-0.308	0.0200	0.463	-0.292	12.9	0.0806	-9.28E-3	-0.0897	0.147	0.489
Chongqing	-0.143	5.11E-3	0.283	-0.0702	9.27	0.0210	-4.84E-3	-0.0140	0.0445	0.557
Guangzhou	-0.332	6.39E-3	0.289	1.48	9.74	0.178	-7.93E-3	-0.0968	-0.150	0.426
Xi'an	-0.124	0.0141	0.0834	-0.141	14.3	0.0483	-6.22E-3	-0.0425	-9.01E-3	0.595
Taiyuan	-0.154	0.0183	0.315	-0.171	12.5	0.0816	-5.68E-3	-0.0795	-0.0169	0.459

	b_{11}	b_{21}	b_{31}	b_{41}	b_{51}	b_{12}	b_{22}	b_{32}	b_{42}	R^2
Jiaozuo	-0.0675	8.27E-4	0.567	0.0265	18.2	0.0342	-2.36E-3	-0.229	0.0159	0.386

The distribution of the best fitting coefficients constrains the weight of each term with respect to its impact on the predicted ozone concentration. However, to make comparisons between the different contributing factors, weighted overall rather than on their magnitude, a weighted fitting is required. First, a universal mean value species-by-species is computed over all of the sites analyzed in this work. Second, this is used to weight each respective species, leading to a mean of 1.0 overall, but a possibility of more/less polluted individual cities having higher/lower mean values. This also accounts for the non-linear terms having multiple magnitudes associated with them across different sites. These weighted coefficients are then used to form a new best fit set of results (**Table 2**), which are solely used to analyze the respective importance of each contributing term and at each urban area, to the overall ability of the model to reproduce the ozone concentration.

Table 2

Weighted Coefficients of Each Term.

	b_{11g}	b_{21g}	b_{31g}	b_{41g}	b_{51g}	b_{12g}	b_{22g}	b_{32g}	b_{42g}
Beijing	0.0465	-0.351	0.756	-0.347	1.78	0.225	0.183	-1.69	0.747
Shanghai	-1.00	2.71	-0.271	-0.122	1.55	1.47	-3.04	-0.131	-3.83E-3
Wuxi	-0.762	1.08	-9.02E-3	0.184	1.13	1.06	-0.982	-0.295	-0.317
Chengdu	-0.325	0.416	0.377	-0.119	1.24	0.451	-1.03	-0.388	0.317
Chongqing	-0.151	0.106	0.230	-0.0286	0.891	0.118	-0.534	-0.0605	0.0961
Guangzhou	-0.351	0.133	0.235	0.601	0.936	1.00	-0.876	-0.419	-0.323
Xi'an	-0.131	0.293	0.0679	-0.0574	1.37	0.270	-0.687	-0.184	-0.0195
Taiyuan	-0.162	0.381	0.257	-0.0696	1.20	0.457	-0.627	-0.344	-0.0366
Jiaozuo	-0.0712	0.0172	0.462	0.0108	1.75	0.192	-0.260	-0.992	0.0343

First, it is observed that the linear UVI term is consistently positive and has a significant magnitude across all cities in the study. This is consistent with the fact that the UV drives the photochemical production via equations 1a, 1h. The remaining species are all important under a specific subset of urban areas, but not consistently across the entire domain. In general, the magnitudes of the non-linear terms are larger than of the linear terms. Furthermore, the non-linear terms involving CO and NO_2 are relevant in most regions, while the terms involving $PM_{2.5}$ and SO_2, both linear and non-linear terms to be relevant in fewer locations, although with a few important exceptions.

The species most connected with ground level ozone concentrations in the literature have historically been NO_2 and VOCs, and herein are reflected by mea-

surements of NO_2 and CO. Although the lifetime of CO is far longer than most other VOCs, it is directly connected with background ozone, as well as being a byproduct of more active VOC chemistry in urban areas, while still being measured at high temporal frequency over long periods of time. It is observed that the linear NO_2 terms only has a significant influence on surface ozone in Beijing and Jiaozuo and a moderate effect in Chengdu, in all cases being positive in nature. The non-linear NO_2 terms are more significant than the linear NO_2 terms respectively in Beijing, Jiaozuo, and to a lesser extent in Chengdu, while the non-linear term is also somewhat important in Guangzhou. In all cases, the non-linear NO_2 terms apply a negative forcing on surface ozone. The positive contributions are consistent with previous studies which reflect the importance of both NO_2 concentrations and UV actinic flux on Ozone levels (Ke Li et al., 2019; W. Wang et al., 2020), while the negative contributions are consistent with the non-linear effects at high actinic fluxes on the titration effects of conditions in which the concentration of NO_x is already very high (Keller et al., 2021).

It is found that the linear CO term plays a rather significant role on the surface ozone in Shanghai and Wuxi, while it also plays a moderate role in Chengdu and Taiyuan. In all of these cases this linear term is also positive, which is consistent with the impacts of CO on consuming OH, leading towards shifts in the HO_x cycle and hence ozone production. This is found to be relevant in those sub-set of areas studied which have a larger number of stations in background environments where stations in Wuxi are located in or close to Taihu Lake, and Shanghai where stations are located in residential blocks, and which otherwise have a generally higher OH level coupled with a high level of CO from large-scale industry and upwind transport. The other subset of places such as in Chengdu and Taiyuan tend to have fewer VOC sources and basin-types of effects allowing for a build-up of OH. This is clearly evidenced by the non-linear CO terms, which are similarly important in the four stations above, although they all tend to be negative. In addition, there is an important non-linear CO term found in Guangzhou, Chongqing, and in Xi'an. These additional urban areas tend to have more complex sources than the other locations, with Guangzhou having intense biomass burning and VOC sources depending on the time of the year, Chongqing having both a rapidly evolving economy plus being an upwind basin receptor from Chengdu, and Xi'an having a considerably growth in both local emissions as well as being upwind of major energy production sources further to its North and West, unique among all of the other locations here. In each of these cases, the secondary production of CO, as well as the effect of CO's reduction of OH in terms of changing the lifetime of HCHO and other smaller VOCs all play important roles. These results are consistent with the fact that Wuxi and Shanghai are the furthest downwind sites in China with a large-scale continuous upwind CO concentration and higher local OH levels, and possibly therefore have the largest possible influence on CO chemistry related to ozone formation, as it has both high OH levels and high CO levels. This is also found to be consistent with the unique status of CO observed in coastal

Jiangsu, Shanghai, and coastal Zhejiang as reported based on the rapid vertical distribution change over this region by Lin et al. (2020), consistent with a possible rapid concentration change associated with surface ozone, due to a measured vertical change in the CO over this region. In Guangzhou the non-linear formation of CO from biogenic VOC oxidation is also important, which may lead to a spike in local CO production which is less smooth and which has had less time to react fully within the urban area.

Although a lot of work has been discussed to look at the issues of aerosols on ozone, analyzing merely the linear term produces a skewed interpretation. It is true that Shanghai and Wuxi have a significant reduction in surface ozone while Guangzhou and Chengdu have a smaller reduction in surface ozone associated with high $PM_{2.5}$, which as explained by Hu et al. (2021) and Wang et al. (2019) would be due to the reduction in surface actinic flux. However, in every one of these cases, the non-linear term shows a positive coefficient which is even larger than the negative coefficient, with the cases of Wuxi, Shanghai and Chengdu being roughly 50% larger and in Guangzhou being nearly 300% larger. In these cases, it is clear that there is a far more complex issue going on involving $PM_{2.5}$ and the reactivity of surface ozone. There are hypotheses which have been explained demonstrating that changes in absorbing aerosols (a sub-component of total $PM_{2.5}$) in turn heats the atmosphere where the aerosol layer is present, stabilizing it, and hence accelerating the formation of ozone through both dynamical and thermodynamic effects (Li et al., 2017; Qu et al., 2021). There are other hypotheses that demonstrate that there could be a significant amount of change in localized deep convection, leading to more intense downwelling of UV during the middle of the day when it is maximized, as compared to more cloud in the morning and evening when the UV flux is otherwise low to begin with, imposing yet another form of non-linearity (Li et al., 2016; Lu, Zhang, et al., 2018; Wang & Prinn, 2000).

Furthermore, SO_2 seems to have a small bit significant negative direct influence in Beijing, while the non-linear term has a larger but positive effect in Beijing. In this case, the behavior of the linear SO_2 is found to generally be similar to the effects of $PM_{2.5}$, and likely are connected with the fact that oxidation and condensation of SO_2 leads to a significant change in the sulfate loading, at which point it would then have a negative impact on ozone formation. There is also a non-linear positive feedback, in which oxidation of SO_2 behaves like CO by reducing OH and therefore accelerating the HO_x cycle (**Equation 1d**), and promoting ozone formation. In Guangzhou the effects of SO_2 are also found to be important, but are completely reversed in magnitude. Here, the rapid formation of sulfate will lead to condensation and layering on top of already sulfur-starved organic particles and thereby tend to increase their absorption (as demonstrated in Wang (2021)). This would lead to the behavior of SO_2 to be more similar to the non-linear impacts of $PM_{2.5}$, while the non-linear effects do not consume as much OH, since the OH tends to be more controlled by the intense amount of biogenic VOC which is in part responsible for the high loadings of organic particles to begin with.

Overall, this may explain that air pollutants and UVR do not influence surface ozone independently, which in turn promotes the idea that interactions between air pollutants and UVR should be taken into account for better quantifying ozone concentration. This is clearly known by the chemical modeling community, which has developed highly complex models to address these phenomena, but which are far too-costly to run at the temporal and spatial frequencies being addressed in this work.

Another critical factor in determining the significance of the fitting is quantifying the ability of the model to match the measurements temporally. As demonstrated in **Figure 2**, ozone simulated by the method employed here is reproduced well in most sites, including Beijing, Chengdu, Chongqing, Xi'an, Taiyuan, and Jiaozuo, with the method capable of capturing both localized temporal trends and well as many of the peaks and troughs. There are some exceptions for extreme events when the measurements are either very high or very low (this will be explained in detail in the next section). Furthermore, there are a few cases in which the results are negative (an example is one daily measurement in Beijing where the model computes a negative value, while the measurement is at about 50 g/m^3). This total number is incredibly small and may be due to errors in the measurements or some other special case in which the ozone concentration is controlled due to an extreme change in a variable not considered in this work.

While the fit is less good in terms of the total match against ozone in Shanghai and Wuxi, the temporal variation is reproduced very well when the ozone concentration is neither extremely high or low. However, the general season-to-season variations tends to be matched well at each site. This is even in Guangzhou, where there is no evident typical seasonal feature according to the available data, which instead is found to match better with some combination of the changes in the Monsoon and local cloudiness, the fit still behaves well under moderate levels of Ozone.

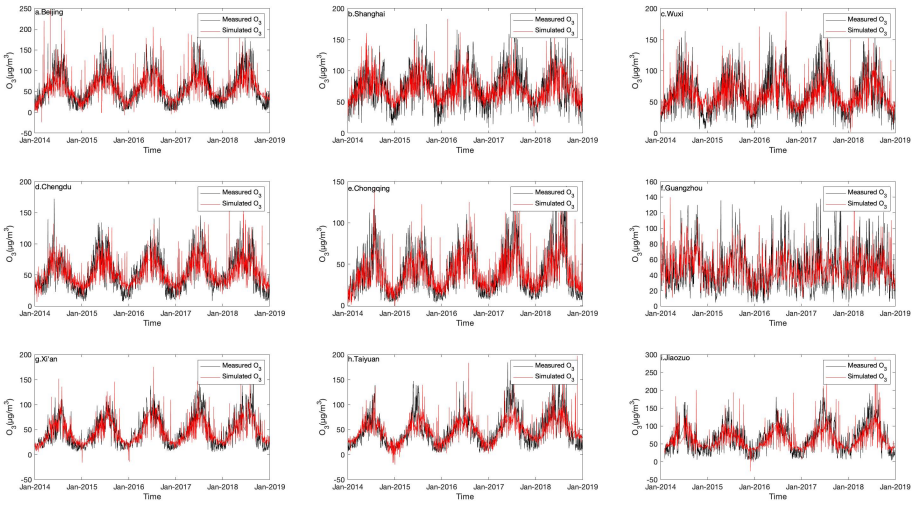

Figure 2. Time series of measured surface ozone (black) and simulated surface ozone (red) at each respective site: a. Beijing; b. Shanghai; c. Wuxi; d. Chengdu; e. Chongqing; f. Guangzhou; g. Xi'an; h. Taiyuan; i. Jiaozuo.

3.2 The Best Fit of Range of Ozone and Its Accuracy

In addition to the model's ability to reproduce the temporal nature of peaks and troughs of ozone, it is essential to capture the magnitude clearly. This is of particular importance under both background and relatively polluted conditions, where linear models tend to do less well. PDFs have been computed from both the measured ozone as well as the modeled ozone, as demonstrated in **Figure 3**. This analysis shows that there is an especially good representation of the magnitude in general in all of the cities above a lower cutoff and below an upper cutoff in ozone concentration. In Guangzhou, the respective lower and upper cutoff are 25 g/m^3 and 90 g/m^3, in Xi'an and Taiyuan the respective lower and upper cutoffs are 10 g/m^3 and 70 g/m^3, and in general elsewhere the respective lower and upper cutoffs are about 10 g/m^3 and 100 g/m^3. In general, the observed goodness of fit range is found to be better in regions which have a drier climatology, with in general the ranges being broader by 25 g/m^3 to 30 g/m^3 or so. This is consistent with the fact that drier regions have fewer issues with clouds and impacts on actinic flux, as well as less non-linear chemistry involving HO_x and water vapor.

A comparison between the ranges of decent fit when using the total linear and non-linear model is generally wider than when using a purely linear model, as demonstrated in the PDFs in Supplemental **Figure A1**. In specific, the range is found to be more accurate in the upper bounds from about 60 to 100 g/m^3.

Furthermore, the non-linear fits are far more smooth, better reproducing the central peak and range far better than the linear fit, with the area between the PDFs over the respective ranges of probability for the non-linear fits being about 0.01 smaller than the respective area between the PDFs for the respective ranges of the linear fits.

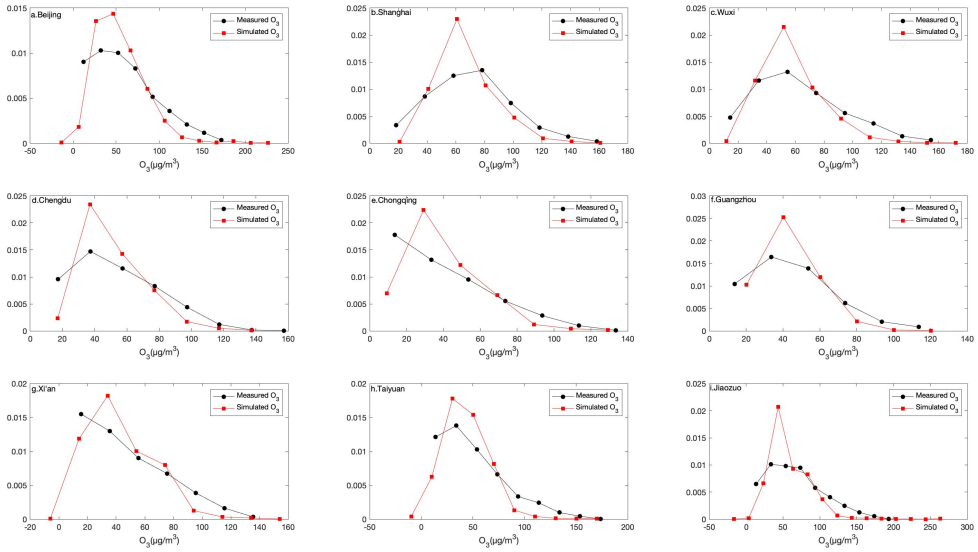

Figure 3. Probability Distribution Functions (PDFs) of measured surface ozone concentrations (black) and simulated surface ozone (red) at the respective sites: a. Beijing; b. Shanghai; c. Wuxi; d. Chengdu; e. Chongqing; f. Guangzhou; g. Xi'an; h. Taiyuan; i. Jiaozuo.

There are sources of error which are observed in the fits at this point are due to a combination of measurement errors (for the inputs used in developing the models as well as the ozone measurements itself) and missing mechanisms (which tend to be more non-linear than represented in this work). There are uncertainties in the surface measurements underlying this work (Hong et al., 2021; Huang et al., 2016), and even larger uncertainties in the remotely sensed measurements (Rodgers, 1990). In addition, such forcings not included in this work but which may also affect the concentration of ozone are non-linear meteorology (i.e. fronts), rapid temperature changes (especially those crossing the 0o threshold), extremely high levels of humidity (RH over 90%), mixing of long-range and local atmospheric air masses, changes in the vertical mixing profile and boundary layer, and strong aerosol layers aloft (An et al., 2007; Chen et al., 2019; Tang et al., 2021). Therefore, it is essential to find a way to choose a range of conditions under which the fitted model is expected to yield a more realistic result. The approach adapted here computes the RMSE of measured

ozone and the bias between the daily model and the measured ozone at each site. The days in which the computed bias is smaller than the measured RMSE are considered to be when the model works well. Additionally, any modeled results which are computed to be smaller than zero also lead to that day's data being not considered.

After these constrains are taken into consideration, the remaining data represents from a minimum of 71% of the total data in Shanghai to a maximum of 78% of the total data in Jiaozuo. Under these new constraints, new PDFs of the remaining measurements of ozone and model fits are given in **Figure 4**. In this case the range of ozone that is capable of being simulated by the model is found to be from 5 to 130 g/m^3 in most of sites, and from 5 to 110 g/m^3 in Chengdu and Chongqing. The statistics of goodness of fit in terms of R^2 and RMSE as done in Section 3.1 are re-applied and show a considerable improvement, with the average value of R^2 increasing from 0.43 to 0.75 and the mean value of RMSE decreasing from 23.1 g/m^3 to 12.1 g/m^3, as displayed in **Table 3**.

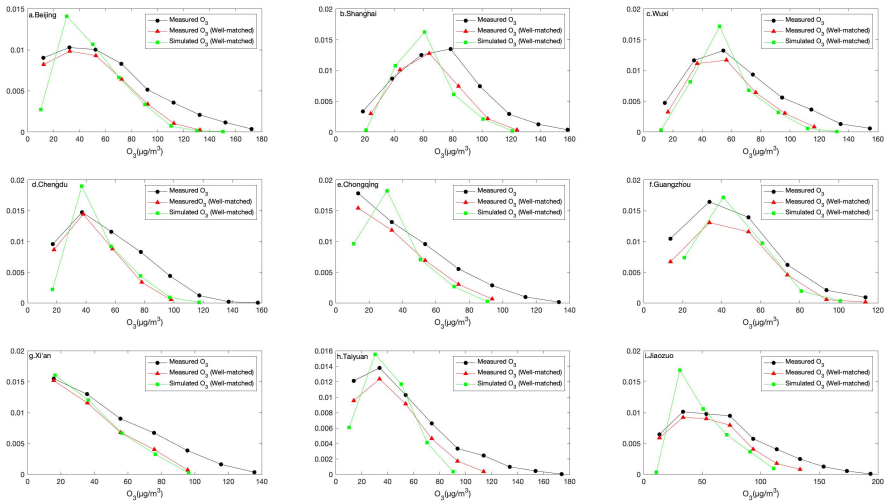

Figure 4. PDFs of all measured surface ozone concentrations (black), well-matched measured surface ozone concentrations (red), and well-matched simulated ozone concentrations (green) at: a. Beijing; b. Shanghai; c. Wuxi; d. Chengdu; e. Chongqing; f. Guangzhou; g. Xi'an; h. Taiyuan; i. Jiaozuo.

Table 3

R^2 and RMSE of the whole fit and the well-matched fit.

	The whole fit	The well-matched fit		
Sites	R^2	RMSE(μg/m^3)	R^2	RMSE(μg/m^3)

	The whole fit	The well-matched fit		
Beijing	0.442	28.5	0.739	14.6
Shanghai	0.231	25.8	0.635	13.8
Wuxi	0.357	25.0	0.670	13.3
Chengdu	0.489	19.8	0.815	9.95
Chongqing	0.557	17.7	0.823	8.80
Guangzhou	0.426	19.4	0.713	10.8
Xi'an	0.595	18.7	0.838	9.77
Taiyuan	0.459	23.5	0.752	11.6
Jiaozuo	0.386	29.9	0.727	16.2

3.3 Ozone Concentrations under Different $PM_{2.5}$ or CO Levels

Due to the fact that aerosols have an impact ozone through changes in the actinic flux as well as the surface temperature due to scattering and absorption, there are expected to be considerable impacts on the ozone levels under both high and low particulate concentration conditions. In this work a classification scheme based on the concentration of $PM_{2.5}$ was used to sort the ozone, with concentrations under 30 g/m^3 considered to be "clean" and concentrations over 120 g/m^3 considered as "highly polluted". PDFs of the UVR and surface ozone under these "clean" and "highly polluted" conditions of $PM_{2.5}$ are presented in **Figure 5** for Xi'an and in **Figure 6** for Beijing. These two urban areas were considered for careful analysis in this section due to the fact that they both exhibit a drier climatology and are therefore expected to have a closer relationship between the $PM_{2.5}$ concentrations, actinic flux, and ozone concentrations.

It is clearly observed that under clean $PM_{2.5}$ conditions there is a very good representation between the total UVI overall distribution and the clean UVI distribution, all the way from 0 to 9 in Xi'an and from 0 to 8 in Beijing. Furthermore, it is evident that there is a very good representation between the total surface ozone distribution and the clean surface ozone distribution, all the way from 0 g/m^3 to about 110 g/m^3 in both Xi'an and Beijing. However, the relationship between total UVI distribution and polluted $PM_{2.5}$ UVI distribution are found to not match as well in both locations, with the values only matching well in Xi'an from 0 to 4, and in Beijing from 0 to 3. Similarly, the relationship between total surface ozone distribution and polluted $PM_{2.5}$ ozone concentrations also are not found to match very well, with the values of overlap only being reasonable from 0 g/m^3 up to 40 g/m^3 in both cities.

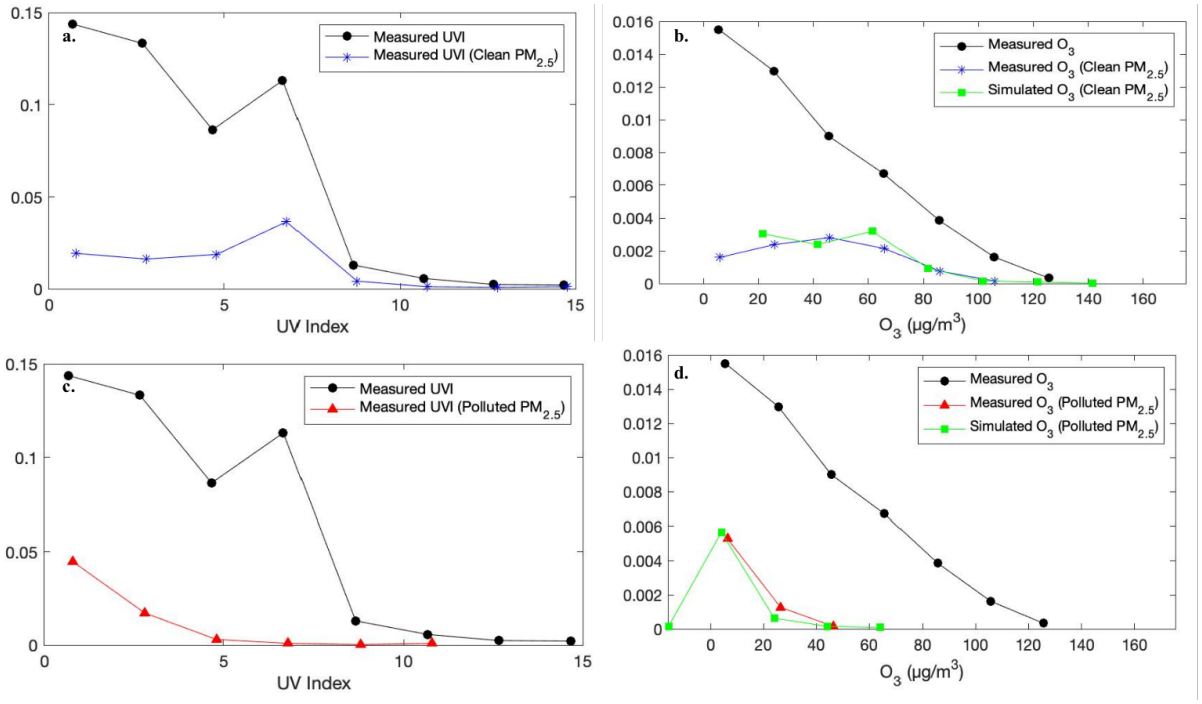

Figure 5. PDFs of all measured UV Index and Ozone values (black), polluted UV Index and Ozone values (red), clean UV Index and Ozone values (blue), and simulated ozone values (green) in Xi'an: a. UV Index at clean $PM_{2.5}$ levels; b. Ozone at clean $PM_{2.5}$ levels; c. UV Index at highly polluted $PM_{2.5}$ levels; and d. Ozone at highly polluted $PM_{2.5}$ levels.

There is also observed to be a small tail in very high ozone conditions in Beijing that occur under highly polluted $PM_{2.5}$ conditions, but does not occur in Xi'an, with concentrations observed in the range from 60 to 110 g/m^3 (in **Figures 6c** and **6d**). This set of low-probability high impact conditions are consistent with the finding that in Beijing, due to both the basin effects and the large amount of absorbing aerosol contribution to total $PM_{2.5}$, that there may be a large amount of net heating and stabilization of the boundary layer, further promoting the formation and accumulation of surface ozone. This result is consistent with the argument above about why Beijing is the only site with a positive coefficient on $PM_{2.5}$.

In general, the distribution and probability of ozone concentration reproduced in this work is similar to that of measurements at different $PM_{2.5}$ levels, except the fit has overestimated O_3 in Guangzhou when $PM_{2.5}$ level is regarded as "heavily polluted". This result, to some extent, suggests the interaction between $PM_{2.5}$ and O_3 was taken into account in the multiple equations computed in this work, while still having deeper complexity in terms of reproducing highly

non-linear meteorological and chemical interactions.

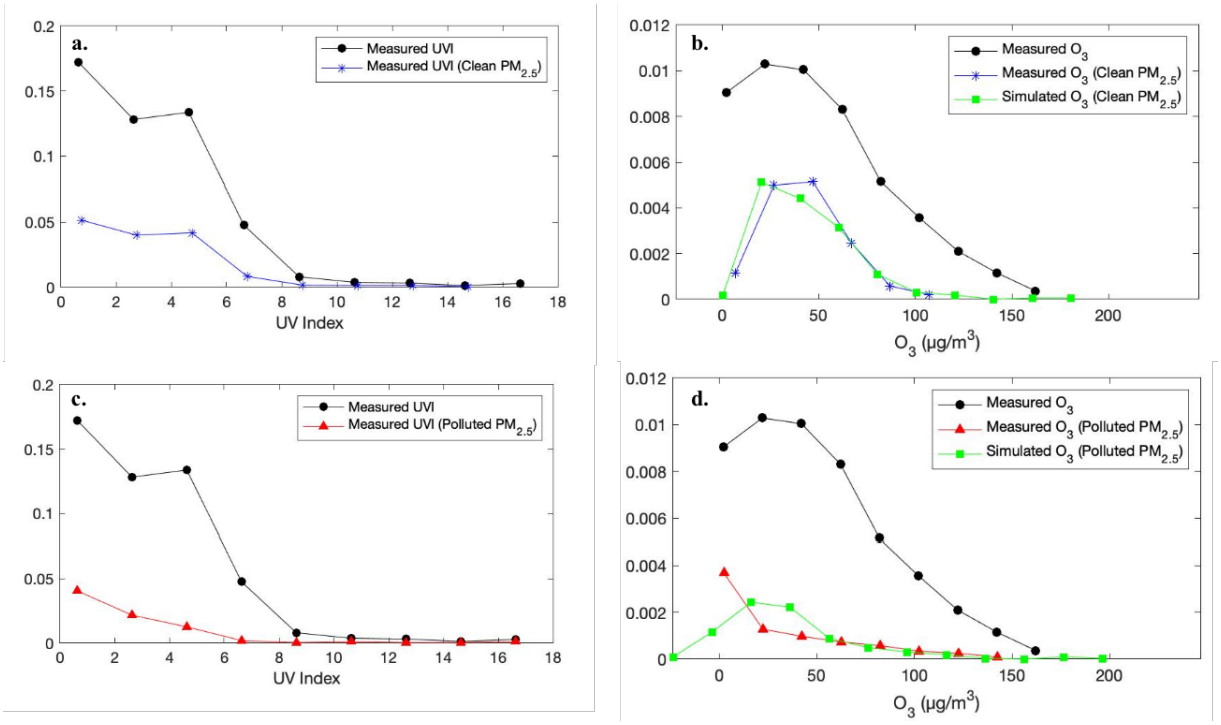

Figure 6. PDFs of all measured UV Index and Ozone values (black), polluted UV Index and Ozone values (red), clean UV Index and Ozone values (blue), and simulated ozone values (green) in Beijing: a. UV Index at clean $PM_{2.5}$ levels; b. Ozone at clean $PM_{2.5}$ levels; c. UV Index at highly polluted $PM_{2.5}$ levels; and d. Ozone at highly polluted $PM_{2.5}$ levels.

The PDFs of surface ozone concentrations were also computed under two different loadings of CO levels, with one is considered to be "clean" (CO with a mass concentration less than 500 g/m^3) and the other considered to be "highly polluted" (CO with a mass concentration over 1500 g/m^3), as displayed in **Figure 7**. Ozone concentrations show an average concentration of 63 g/m^3 and a range from 24 to 111 g/m^3 under clean conditions and an average concentration of 31 g/m^3 and a range from 5 to 110 g/m^3 under highly polluted CO levels. This finding is consistent with the idea that under higher concentrations of CO, the HO_x cycle would be disrupted, with more photolysis required to obtain a similar level of OH, due to the fact that CO acts to both suppress OH, as well as being a surrogate of other larger VOC oxidation pathways, which in turn may have also acted to suppress OH.

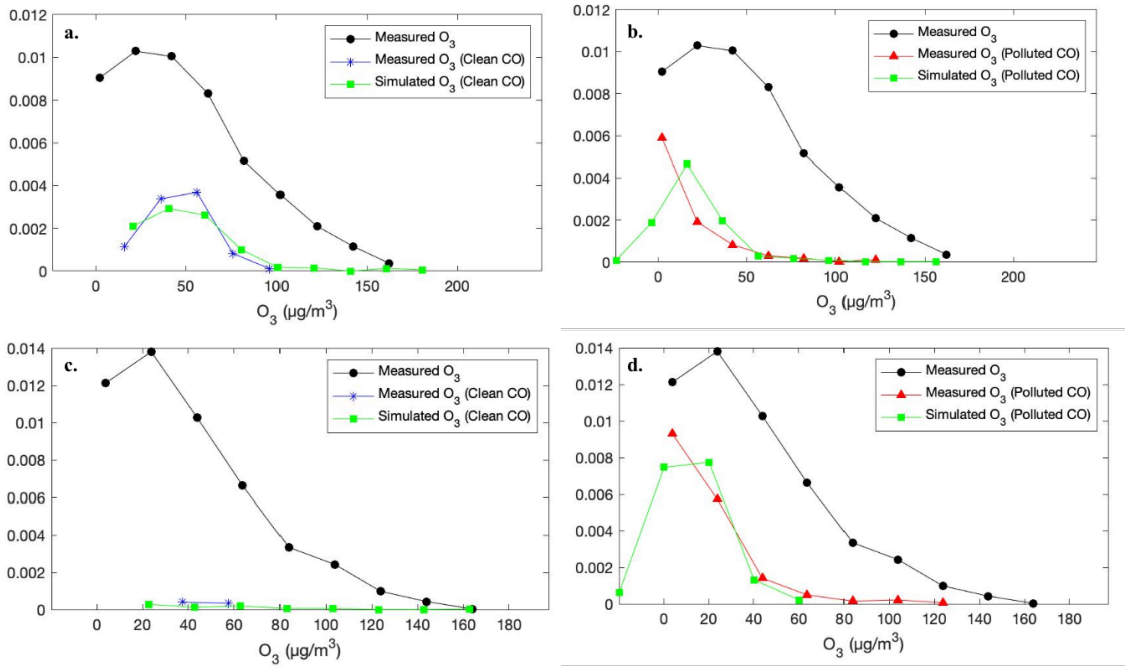

Figure 7. PDFs of all measured Ozone values (black), polluted Ozone values (red), clean Ozone values (blue), and simulated ozone values (green): a. Ozone at clean CO levels in Beijing; b. Ozone at polluted CO levels in Beijing; c. Ozone at clean CO levels in Taiyuan; and d. Ozone at polluted CO levels in Taiyuan.

4 Conclusions and Discussions

This work has built a multiple regression equation of surface ozone using a combination of measured air pollutant concentrations ($PM_{2.5}$, CO, NO_2, and SO_2) and remotely sensed ultraviolet index (UVI). Furthermore, non-linear terms between each air pollutant and UVI has also been built into a multiple regression equation. All models are at high frequency based on daily measurements, and their fits evaluated against daily measurements of surface ozone. Overall, the measurement fit was found to have an R^2 over 0.43 and RMSE smaller than 24 g/m^3 in most sites investigated. This is consistent with the fit capturing both localized temporal trends and well as many of the peaks and troughs. Even in sites where the temporal fit does not seem very good, the seasonal variation is still well captured in terms of larger-scale peaks and troughs. It is worth noting that in Guangzhou, while surface ozone shows no evident season-to-season features, the non-linear timing and impact of the Monsoon and other non-linear tropical forcings are still reasonably well represented.

Secondly, the impact of extreme values in terms of time and range are explored at each site. It is determined that so long as the ozone is within a central range,

varying from 5 g/m^3 to 120 g/m^3 of ozone across the different sites, that the overall fit is found to be far better in terms of both space and time, with the overall R^2 increased to over 0.64 to RMSE decreased to under 14 g/m^3 at all sites. This is an excellent result for 24-hour ozone concentration prediction, which is even better than other big-data approaches, which tend to only focus on. Maximum 8 hourly ozone, and still have an RMSE of 20 g/m^3 and higher (Wei et al., 2021).

Thirdly, the driving factors behind the various fits and ranges were successfully analyzed, considering both clean and heavily polluted levels of $PM_{2.5}$ and CO respectively. It was found that under clean $PM_{2.5}$ conditions, that UVI and ozone both were higher than under heavily polluted $PM_{2.5}$ conditions, with a difference in UVI average of 2 and a difference in Ozone average of 23 g/m^3. In the case of heavily polluted CO conditions, the average Ozone was found to be 31 g/m^3 while in the case of clean CO conditions, the average Ozone was found to be 63 g/m^3. These indicate clearly that $PM_{2.5}$ and CO both represent extreme forcings that contribute to surface Ozone, and that these are two important factors in particular in urban areas found under drier climate conditions. These results are found to be consistent with theory, where changes in UV radiation reaching at surface due to aerosol extinction led to changes in photochemistry. Furthermore, this is consistent with the theory that higher CO levels would significantly impact the HO_x cycle.

Fourthly, the work shows clearly that UVI is the single most important overall species in terms of total contribution to the overall surface ozone conditions. This is true for both its direct term, as well as its non-linear terms, with CO and NO_2 in a larger number of urban areas, and $PM_{2.5}$ and SO_2 in fewer urban areas. These results show clearly that solar ultraviolet radiation, together with longer-lived air pollutants contribute a significant amount to lot to surface ozone, without needing to directly consider various meteorological variables or VOCs.

Acknowledgments

We would like to gratefully acknowledge the data and measurements provided by the entire OMI NO_2 team (https://disc.gsfc.nasa.gov/datasets/OMUVBG_003/summary), and the China National Environmental Monitoring Center (https://doi.org/10.6084/m9.figshare.17702462). All data used in this work and all model results not otherwise provided in tables and supplemental tables can be found at (https://doi.org/10.6084/m9.figshare.17702462). Financial support was obtained from the Chinese National Young Thousand Talents Program (Project 41180002) and the Chinese National Natural Science Foundation (Project 41030028; Project 42075147).

Open Research

All underlying data, processed data, models, and results are freely available for download at (https://doi.org/10.6084/m9.figshare.17702462).

References

https://doi.org/10.1029/2019jd031971

https://doi.org/10.1007/s00376-007-0573-0

https://doi.org/10.1016/j.rse.2011.11.010

https://doi.org/10.1029/1998gl900013

https://doi.org/10.3390/ijerph17218105

https://doi.org/10.1016/j.envpol.2018.10.117

https://doi.org/10.5194/acp-19-6125-2019

https://doi.org/10.1088/1748-9326/9/11/114018

https://doi.org/10.5194/acp-11-7629-2011

https://doi.org/10.1029/2011gl047417

https://doi.org/10.1002/2013jd019912

https://doi.org/10.1002/2016gl067745

https://doi.org/10.1562/2004-11-19-RN-375

https://doi.org/10.1029/2019gl082666

https://doi.org/10.1029/2012gl052064

https://doi.org/10.1016/j.jes.2020.09.036

https://doi.org/10.1038/srep44851

https://doi.org/10.1016/j.scitotenv.2021.148624

https://doi.org/10.1016/j.partic.2013.10.005

https://doi.org/10.1016/j.rse.2016.04.001

https://doi.org/10.1016/j.envpol.2011.04.025

10.5067/Aura/OMI/DATA2028

https://doi.org/10.1038/s41598-019-55759-7

https://doi.org/10.1016/j.atmosenv.2015.08.087

https://doi.org/10.1073/pnas.1812168116

https://doi.org/10.1038/s41561-019-0464-x

https://doi.org/10.1016/j.atmosenv.2015.10.075

https://doi.org/10.1007/s10311-021-01265-0

https://doi.org/10.1002/jgrd.50659

https://doi.org/10.1016/j.envint.2015.10.016
https://doi.org/10.1088/1748-9326/abaa7a
https://doi.org/10.1016/j.scitotenv.2019.04.121
https://doi.org/10.1016/s0022-4073(03)00231-0
https://doi.org/10.5194/acp-20-6323-2020
https://doi.org/10.1021/acs.estlett.8b00366
https://doi.org/10.1021/acs.estlett.0c00171
https://doi.org/10.1029/2018JD028912
https://doi.org/10.1016/j.apr.2019.01.007
https://doi.org/10.1029/2004gl022228
https://doi.org/10.1126/science.1064034
https://doi.org/10.1002/2015gl064037
https://doi.org/10.1038/nature06059
https://doi.org/10.1038/s41612-020-00131-0
https://doi.org/10.1016/j.scitotenv.2021.147740
https://doi.org/10.1039/c0pp90041a
https://doi.org/10.5194/acp-17-9485-2017
https://doi.org/10.1029/2002JD002893
https://doi.org/10.1029/2000jd900263
https://doi.org/10.1016/j.partic.2014.06.013
https://doi.org/10.1016/j.scitotenv.2019.01.227
https://doi.org/10.1016/j.scitotenv.2008.01.059
https://doi.org/10.1029/2021ef002167
https://doi.org/10.5194/acp-20-15401-2020
https://doi.org/10.1029/2021gl094300
https://doi.org/10.1016/j.scitotenv.2016.10.081
https://doi.org/10.1093/nsr/nwaa032
https://doi.org/10.1073/pnas.1916775117
https://doi.org/10.1029/2008gl036607
https://doi.org/10.1016/j.ecolind.2019.105889
https://doi.org/10.1088/1748-9326/2/4/045027

https://doi.org/10.1007/s13351-014-4089-0

Abdi-Oskouei, M., Carmichael, G., Christiansen, M., Ferrada, G., Roozitalab, B., Sobhani, N., Wade, K., Czarnetzki, A., Pierce, R. B., Wagner, T., & Stanier, C. (2020). Sensitivity of Meteorological Skill to Selection of WRF-Chem Physical Parameterizations and Impact on Ozone Prediction During the Lake Michigan Ozone Study (LMOS). *Journal of Geophysical Research: Atmospheres*, *125*(5). An, J., Cheng, X., Qu, Y., & Chen, Y. (2007). Influence of vertical eddy diffusivity parameterization on daily and monthly mean concentrations of O3 and NOy. *Advances in Atmospheric Sciences*, *24*(4), 573-580. Bak, J., Kim, J. H., Spurr, R. J. D., Liu, X., & Newchurch, M. J. (2012). Sensitivity study of ozone retrieval from UV measurements on geostationary platforms. *Remote Sensing of Environment*, *118*, 309-319. Belan, B. D., & Sklyadneva, T. K. (1999, November). Influence of solar radiation on the variation of ozone concentration in the ground atmospheric layer. In *Sixth International Symposium on Atmospheric and Ocean Optics* (Vol. 3983, pp. 76-82). International Society for Optics and Photonics.Brasseur, G. P., Kiehl, J. T., Müller, J.-F., Schneider, T., Granier, C., Tie, X., & Hauglustaine, D. (1998). Past and future changes in global tropospheric ozone: Impact on radiative forcing. *Geophysical Research Letters*, *25*(20), 3807-3810. Cadet, J. M., Bencherif, H., Cadet, N., Lamy, K., Portafaix, T., Belus, M., Brogniez, C., Auriol, F., Metzger, J. M., & Wright, C. Y. (2020). Solar UV Radiation in the Tropics: Human Exposure at Reunion Island (21 degrees S, 55 degrees E) during Summer Outdoor Activities. *Int J Environ Res Public Health*, *17*(21). Chen, Z., Zhuang, Y., Xie, X., Chen, D., Cheng, N., Yang, L., & Li, R. (2019). Understanding long-term variations of meteorological influences on ground ozone concentrations in Beijing During 2006-2016. *Environ Pollut*, *245*, 29-37. Cheng, J., Su, J., Cui, T., Li, X., Dong, X., Sun, F., Yang, Y., Tong, D., Zheng, Y., Li, Y., Li, J., Zhang, Q., & He, K. (2019). Dominant role of emission reduction in PM_{2.5} air quality improvement in Beijing during 2013–2017: a model-based decomposition analysis. *Atmospheric Chemistry and Physics*, *19*(9), 6125-6146. Cohen, J. B. (2014). Quantifying the occurrence and magnitude of the Southeast Asian fire climatology. *Environmental Research Letters*, *9*(11). Cohen, J. B., & Prinn, R. G. (2011). Development of a fast, urban chemistry metamodel for inclusion in global models. *Atmospheric Chemistry and Physics*, *11*(15), 7629-7656. Cohen, J. B., Prinn, R. G., & Wang, C. (2011). The impact of detailed urban-scale processing on the composition, distribution, and radiative forcing of anthropogenic aerosols. *Geophysical Research Letters*, *38*(10), n/a-n/a. Cohen, J. B., & Wang, C. (2014). Estimating global black carbon emissions using a top-down Kalman Filter approach. *Journal of Geophysical Research: Atmospheres*, *119*(1), 307-323. Deng, W., Cohen, J. B., Wang, S., & Lin, C. (2021). Improving the understanding between climate variability and observed extremes of global NO2 over the past 15 years. *Environmental Research Letters*, *16*(5), 054020.Ding, A. J., Huang, X., Nie, W., Sun, J. N., Kerminen, V. M., Petäjä, T., Su, H., Cheng, Y. F., Yang, X. Q., Wang, M. H., Chi, X. G., Wang, J. P., Virkkula, A., Guo, W. D., Yuan, J., Wang, S. Y., Zhang, R. J., Wu, Y. F., Song, Y., . . . Fu, C. B.

(2016). Enhanced haze pollution by black carbon in megacities in China. *Geophysical Research Letters*, *43*(6), 2873-2879. Engelsen, O., Brustad, M., Aksnes, L., & Lund, E. (2005). Daily duration of vitamin D synthesis in human skin with relation to latitude, total ozone, altitude, ground cover, aerosols and cloud thickness. *Photochem Photobiol*, *81*(6), 1287-1290. Guo, J., Li, Y., Cohen, J. B., Li, J., Chen, D., Xu, H., Liu, L., Yin, J., Hu, K., & Zhai, P. (2019). Shift in the Temporal Trend of Boundary Layer Height in China Using Long-Term (1979–2016) Radiosonde Data. *Geophysical Research Letters*, *46*(11), 6080-6089. Hill, S., & Ming, Y. (2012). Nonlinear climate response to regional brightening of tropical marine stratocumulus. *Geophysical Research Letters*, *39*(15). Holben, B. N., Eck, T. F., Slutsker, I. a., Tanre, D., Buis, J. P., Setzer, A., Vermote, E., Reagan, J. A., Kaufman, Y. J., & Nakajima, T. (1998). AERONET—A federated instrument network and data archive for aerosol characterization. *Remote Sensing of Environment*, *66*(1), 1-16. Hong, Q., Liu, C., Hu, Q., Xing, C., Tan, W., Liu, T., & Liu, J. (2021). Vertical distributions of tropospheric SO2 based on MAX-DOAS observations: Investigating the impacts of regional transport at different heights in the boundary layer. *Journal of Environmental Sciences*, *103*, 119-134. Hu, B., Zhao, X., Liu, H., Liu, Z., Song, T., Wang, Y., Tang, L., Xia, X., Tang, G., Ji, D., Wen, T., Wang, L., Sun, Y., & Xin, J. (2017). Quantification of the impact of aerosol on broadband solar radiation in North China. *Sci Rep*, *7*, 44851. Hu, J., Zhao, T., Liu, J., Cao, L., Xia, J., Wang, C., Zhao, X., Gao, Z., Shu, Z., & Li, Y. (2021). Nocturnal surface radiation cooling modulated by cloud cover change reinforces PM2.5 accumulation: Observational study of heavy air pollution in the Sichuan Basin, Southwest China. *Sci Total Environ*, *794*, 148624. Huang, G., Cheng, T., Zhang, R., Tao, J., Leng, C., Zhang, Y., Zha, S., Zhang, D., Li, X., & Xu, C. (2014). Optical properties and chemical composition of PM 2.5 in Shanghai in the spring of 2012. *Particuology*, *13*, 52-59. Huang, G., Li, X., Huang, C., Liu, S., Ma, Y., & Chen, H. (2016). Representativeness errors of point-scale ground-based solar radiation measurements in the validation of remote sensing products. *Remote Sensing of Environment*, *181*, 198-206. Huo, H., Zhang, Q., He, K., Yao, Z., Wang, X., Zheng, B., Streets, D. G., Wang, Q., & Ding, Y. (2011). Modeling vehicle emissions in different types of Chinese cities: importance of vehicle fleet and local features. *Environ Pollut*, *159*(10), 2954-2960. Jari Hovila, Antii Arola, and Johanna Tamminen (2014), OMI/Aura Surface UVB Irradiance and Erythemal Dose Daily L2 Global Gridded 0.25 degree x 0.25 degree V3, NASA Goddard Space Flight Center, Goddard Earth Sciences Data and Information Services Center (GES DISC), Accessed: [*December, 2021*], Kajino, M., Hayashida, S., Sekiyama, T. T., Deushi, M., Ito, K., & Liu, X. (2019). Detectability assessment of a satellite sensor for lower tropospheric ozone responses to its precursors emission changes in East Asian summer. *Sci Rep*, *9*(1), 19629. Karagulian, F., Belis, C. A., Dora, C. F. C., Prüss-Ustün, A. M., Bonjour, S., Adair-Rohani, H., & Amann, M. (2015). Contributions to cities' ambient particulate matter (PM): A systematic review of local source contributions at global level. *Atmospheric Environment*, *120*, 475-483. Keller, C. A., Evans, M. J., Knowland, K. E., Hasenkopf, C. A., Modekurty, S., Lucchesi, R. A., Oda, T., Franca, B. B., Mandarino, F. C., &

Díaz Suárez, M. V. (2021). Global impact of COVID-19 restrictions on the surface concentrations of nitrogen dioxide and ozone. *Atmospheric Chemistry and Physics*, *21*(5), 3555-3592 Li, K., Jacob, D. J., Liao, H., Shen, L., Zhang, Q., & Bates, K. H. (2019). Anthropogenic drivers of 2013-2017 trends in summer surface ozone in China. *Proc Natl Acad Sci U S A*, *116*(2), 422-427. Li, K., Jacob, D. J., Liao, H., Zhu, J., Shah, V., Shen, L., Bates, K. H., Zhang, Q., & Zhai, S. (2019). A two-pollutant strategy for improving ozone and particulate air quality in China. *Nature Geoscience*, *12*(11), 906-910. Li, M., Song, Y., Mao, Z., Liu, M., & Huang, X. (2016). Impacts of thermal circulations induced by urbanization on ozone formation in the Pearl River Delta region, China. *Atmospheric Environment*, *127*, 382-392. Li, M., Yu, S., Chen, X., Li, Z., Zhang, Y., Wang, L., Liu, W., Li, P., Lichtfouse, E., Rosenfeld, D., & Seinfeld, J. H. (2021). Large scale control of surface ozone by relative humidity observed during warm seasons in China. *Environmental Chemistry Letters*, *19*(6), 3981-3989. Li, Y., Lau, A. K. H., Fung, J. C. H., Zheng, J., & Liu, S. (2013). Importance of NOx control for peak ozone reduction in the Pearl River Delta region. *Journal of Geophysical Research: Atmospheres*, *118*(16), 9428-9443. Li, Z., Guo, J., Ding, A., Liao, H., Liu, J., Sun, Y., Wang, T., Xue, H., Zhang, H., & Zhu, B. (2017). Aerosol and boundary-layer interactions and impact on air quality. *NATIONAL SCIENCE REVIEW*, *4*(6), 810-833. Liang, C. S., Duan, F. K., He, K. B., & Ma, Y. L. (2016). Review on recent progress in observations, source identifications and countermeasures of PM2.5. *Environ Int*, *86*, 150-170. Liang, M., Zhang, Y., Ma, Q., Yu, D., Chen, X., & Cohen, J. B. (2021). Dramatic decline of observed atmospheric CO2 and CH4 during the COVID-19 lockdown over the Yangtze River Delta of China. *Journal of Environmental Sciences*. Liao, K. J. T., Efthimios; Napelenok, Sergey L.; Manomaiphiboon, Kasemsan; Woo, Jun Hun; Amar, Praveen; He, Shan; Russell, Armistead G.. (2008). Current and Future Linked Responses of Ozone and PM2.5 to Emission Controls. *Environmental Science and Technology*, *42*(13), 6. Lin, C., Cohen, J. B., Wang, S., Lan, R., & Deng, W. (2020). A new perspective on the spatial, temporal, and vertical distribution of biomass burning: quantifying a significant increase in CO emissions. *Environmental Research Letters*, *15*(10). Liu, Q., Liu, T., Chen, Y., Xu, J., Gao, W., Zhang, H., & Yao, Y. (2019). Effects of aerosols on the surface ozone generation via a study of the interaction of ozone and its precursors during the summer in Shanghai, China. *Sci Total Environ*, *675*, 235-246. Liu, X., Chance, K., Sioris, C. E., Spurr, R. J. D., Kurosu, T. P., Martin, R. V., & Newchurch, M. J. (2005). Ozone profile and tropospheric ozone retrievals from the Global Ozone Monitoring Experiment: Algorithm description and validation. *Journal of Geophysical Research: Atmospheres*, *110*(D20).Liu, X., Newchurch, M. J., Loughman, R., & Bhartia, P. K. (2004). Errors resulting from assuming opaque Lambertian clouds in TOMS ozone retrieval. *Journal of Quantitative Spectroscopy and Radiative Transfer*, *85*(3-4), 337-365. Liu, Y., & Wang, T. (2020). Worsening urban ozone pollution in China from 2013 to 2017 – Part 2: The effects of emission changes and implications for multi-pollutant control. *Atmospheric Chemistry and Physics*, *20*(11), 6323-6337. Lu, X., Hong, J., Zhang, L., Cooper, O. R., Schultz, M. G., Xu, X., Wang, T., Gao, M.,

Zhao, Y., & Zhang, Y. (2018). Severe Surface Ozone Pollution in China: A Global Perspective. *Environmental Science & Technology Letters*, *5*(8), 487-494. Lu, X., Zhang, L., Liu, X., Gao, M., Zhao, Y., & Shao, J. (2018). Lower tropospheric ozone over India and its linkage to the South Asian monsoon. *Atmospheric Chemistry and Physics*, *18*(5), 3101-3118. Lu, X., Zhang, L., Wang, X., Gao, M., Li, K., Zhang, Y., Yue, X., & Zhang, Y. (2020). Rapid Increases in Warm-Season Surface Ozone and Resulting Health Impact in China Since 2013. *Environmental Science & Technology Letters*, *7*(4), 240-247. Martin, R. V. (2008). Satellite remote sensing of surface air quality. *Atmospheric Environment*, *42*(34), 7823-7843 Miyazaki, K., Sekiya, T., Fu, D., Bowman, K. W., Kulawik, S. S., Sudo, K., Walker, T., Kanaya, Y., Takigawa, M., Ogochi, K., Eskes, H., Boersma, K. F., Thompson, A. M., Gaubert, B., Barre, J., & Emmons, L. K. (2019). Balance of Emission and Dynamical Controls on Ozone During the Korea-United States Air Quality Campaign From Multiconstituent Satellite Data Assimilation. *J Geophys Res Atmos*, *124*(1), 387-413. Pan, L., Xu, J., Tie, X., Mao, X., Gao, W., & Chang, L. (2019). Long-term measurements of planetary boundary layer height and interactions with PM2.5 in Shanghai, China. *Atmospheric Pollution Research*, *10*(3), 989-996. Prinn, R. G., Huang, J., Weiss, R. F., Cunnold, D. M., Fraser, P. J., Simmonds, P. G., McCulloch, A., Harth, C., Reimann, S., Salameh, P., O'Doherty, S., Wang, R. H. J., Porter, L. W., Miller, B. R., & Krummel, P. B. (2005). Evidence for variability of atmospheric hydroxyl radicals over the past quarter century. *Geophysical Research Letters*, *32*(7), n/a-n/a. Qu, Y., Voulgarakis, A., Wang, T., Kasoar, M., Wells, C., Yuan, C., Varma, S., & Mansfield, L. (2021). A study of the effect of aerosols on surface ozone through meteorology feedbacks over China. *Atmospheric Chemistry and Physics*, *21*(7), 5705-5718 Ramanathan, V., Crutzen, P. J., Kiehl, J. T., & Rosenfeld, D. (2001). Aerosols, climate, and the hydrological cycle. *Science*, *294*(5549), 2119-2124. Rap, A., Richards, N. A. D., Forster, P. M., Monks, S. A., Arnold, S. R., & Chipperfield, M. P. (2015). Satellite constraint on the tropospheric ozone radiative effect. *Geophysical Research Letters*, *42*(12), 5074-5081. Rodgers, C. D. (1990). Characterization and error analysis of profiles retrieved from remote sounding measurements. *Journal of Geophysical Research: Atmospheres*, *95*(D5), 5587-5595.Seinfeld, J. H., Kleindienst, T. E., Edney, E. O., & Cohen, J. B. (2003). Aerosol growth in a steady-state, continuous flow chamber: Application to studies of secondary aerosol formation. *Aerosol Science & Technology*, *37*(9), 728-734. Seinfeld, J. H., & Pandis, S. N. (1998). *From Air Pollution to Climate Change. Atmospheric Chemistry and Physics.* Sitch, S., Cox, P. M., Collins, W. J., & Huntingford, C. (2007). Indirect radiative forcing of climate change through ozone effects on the land-carbon sink. *Nature*, *448*(7155), 791-794. Skeie, R. B., Myhre, G., Hodnebrog, Ø., Cameron-Smith, P. J., Deushi, M., Hegglin, M. I., Horowitz, L. W., Kramer, R. J., Michou, M., Mills, M. J., Olivié, D. J. L., Connor, F. M. O., Paynter, D., Samset, B. H., Sellar, A., Shindell, D., Takemura, T., Tilmes, S., & Wu, T. (2020). Historical total ozone radiative forcing derived from CMIP6 simulations. *npj Climate and Atmospheric Science*, *3*(1). Steinbrecht, W., McGee, T. J., Twigg, L. W., Claude, H., Schönenborn, F., Sumnicht, G. K., & Silbert, D.

(2009). Intercomparison of stratospheric ozone and temperature profiles during the October 2005 Hohenpeißenberg Ozone Profiling Experiment (HOPE). *Atmospheric Measurement Techniques*, *2*(1), 125-145. Tang, G., Liu, Y., Huang, X., Wang, Y., Hu, B., Zhang, Y., Song, T., Li, X., Wu, S., Li, Q., Kang, Y., Zhu, Z., Wang, M., Wang, Y., Li, T., Li, X., & Wang, Y. (2021). Aggravated ozone pollution in the strong free convection boundary layer. *Sci Total Environ*, *788*, 147740. Tang, X., Wilson, S. R., Solomon, K. R., Shao, M., & Madronich, S. (2011). Environmental effects of ozone depletion and its interactions with climate change: 2010 assessment. Introduction. *Photochem Photobiol Sci*, *10*(2), 174. Tao, J., Zhang, L., Cao, J., & Zhang, R. (2017). A review of current knowledge concerning PM_{2. 5} chemical composition, aerosol optical properties and their relationships across China. *Atmospheric Chemistry and Physics*, *17*(15), 9485-9518. Tie, X., Geng, F., Peng, L., Gao, W., & Zhao, C. (2009). Measurement and modeling of O3 variability in Shanghai, China: Application of the WRF-Chem model. *Atmospheric Environment*, *43*(28), 4289-4302. Visser, A. J., Boersma, K. F., Ganzeveld, L. N., & Krol, M. C. (2019). European NO x emissions in WRF-Chem derived from OMI: impacts on summertime surface ozone. *Atmospheric Chemistry and Physics*, *19*(18), 11821-11841. von Kuhlmann, R., Lawrence, M. G., Crutzen, P. J., & Rasch, P. J. (2003). A model for studies of tropospheric ozone and nonmethane hydrocarbons: Model description and ozone results. *Journal of Geophysical Research: Atmospheres*, *108*(D9). , 2003 Wang, C., & Prinn, R. G. (2000). On the roles of deep convective clouds in tropospheric chemistry. *Journal of Geophysical Research: Atmospheres*, *105*(D17), 22269-22297. Wang, H., Yang, T., & Wang, Z. (2020). Development of a coupled aerosol lidar data quality assurance and control scheme with Monte Carlo analysis and bilateral filtering. *Science of The Total Environment*, *728*, 138844 Wang, H., Zhu, B., Zhang, Z., An, J., & Shen, L. (2015). Mixing state of individual carbonaceous particles during a severe haze episode in January 2013, Nanjing, China. *Particuology*, *20*, 16-23. Wang, P., Guo, H., Hu, J., Kota, S. H., Ying, Q., & Zhang, H. (2019). Responses of PM2.5 and O3 concentrations to changes of meteorology and emissions in China. *Sci Total Environ*, *662*, 297-306. Wang, Q., Han, Z., Wang, T., & Zhang, R. (2008). Impacts of biogenic emissions of VOC and NOx on tropospheric ozone during summertime in eastern China. *Sci Total Environ*, *395*(1), 41-49. Wang, S., Cohen, J. B., Deng, W., Qin, K., & Guo, J. (2021). Using a New Top-Down Constrained Emissions Inventory to Attribute the Previously Unknown Source of Extreme Aerosol Loadings Observed Annually in the Monsoon Asia Free Troposphere. *Earth's Future*, *9*(7). Wang, S., Cohen, J. B., Lin, C., & Deng, W. (2020). Constraining the relationships between aerosol height, aerosol optical depth and total column trace gas measurements using remote sensing and models. *Atmospheric Chemistry and Physics*, *20*(23), 15401-15426. Wang, S., Wang, X., Cohen, J. B., & Qin, K. (2021). Inferring Polluted Asian Absorbing Aerosol Properties Using Decadal Scale AERONET Measurements and a MIE Model. *Geophysical Research Letters*, *48*(20). Wang, T., Xue, L., Brimblecombe, P., Lam, Y. F., Li, L., & Zhang, L. (2017). Ozone pollution in China: A review of concentrations, meteorological influences, chemical pre-

cursors, and effects. *Sci Total Environ*, *575*, 1582-1596. Wang, W., Parrish, D. D., Li, X., Shao, M., Liu, Y., Mo, Z., Lu, S., Hu, M., Fang, X., & Wu, Y. (2020). Exploring the drivers of the increased ozone production in Beijing in summertime during 2005–2016. *Atmospheric Chemistry and Physics*, *20*(24), 15617-15633 Wang, Y., Gao, W., Wang, S., Song, T., Gong, Z., Ji, D., Wang, L., Liu, Z., Tang, G., Huo, Y., Tian, S., Li, J., Li, M., Yang, Y., Chu, B., Petaja, T., Kerminen, V. M., He, H., Hao, J., . . . Zhang, Y. (2020). Contrasting trends of PM2.5 and surface-ozone concentrations in China from 2013 to 2017. *Natl Sci Rev*, *7*(8), 1331-1339. Wei, J., Li, Z., Li, K., Dickerson, R. R., Pinker, R. T., Wang, J., Liu, X., Sun, L., Xue, W., & Cribb, M. (2021). Full-coverage mapping and spatiotemporal variations of ground-level ozone (O3) pollution from 2013 to 2020 across China. Remote Sensing of Environment, 112775.World Health Organization (WHO). (2020). *Global Solar UV Index - A Practical Guide* Wu, J., Bei, N., Hu, B., Liu, S., Wang, Y., Shen, Z., Li, X., Liu, L., Wang, R., Liu, Z., Cao, J., Tie, X., Molina, L. T., & Li, G. (2020). Aerosol-photolysis interaction reduces particulate matter during wintertime haze events. *Proc Natl Acad Sci U S A*, *117*(18), 9755-9761. Wu, S., Duncan, B. N., Jacob, D. J., Fiore, A. M., & Wild, O. (2009). Chemical nonlinearities in relating intercontinental ozone pollution to anthropogenic emissions. *Geophysical Research Letters*, *36*(5). Xu, G., Ren, X., Xiong, K., Li, L., Bi, X., & Wu, Q. (2020). Analysis of the driving factors of PM2.5 concentration in the air: A case study of the Yangtze River Delta, China. *Ecological Indicators*, *110*. Zhang, Q., Streets, D. G., He, K., & Klimont, Z. (2007). Major components of China's anthropogenic primary particulate emissions. *Environmental Research Letters*, *2*(4). Zhang, Y., Zhang, Q., Leng, C., Zhang, D., Cheng, T., Tao, J., Zhang, R., & He, Q. (2015). Evolution of aerosol vertical distribution during particulate pollution events in Shanghai. *Journal of Meteorological Research*, *29*(3), 385-399.